

An Integral Equation Approach to Effective Interactions between Polymers in Solution<sup>†</sup>V. Krakoviack,<sup>\*,‡</sup> B. Rotenberg,<sup>§,||</sup> and J.-P. Hansen<sup>§</sup>

Laboratoire de Chimie, École Normale Supérieure de Lyon, 46 Allée d'Italie, 69364 Lyon Cedex 07, France,  
 Department of Chemistry, University of Cambridge, Lensfield Road, Cambridge CB2 1EW, United Kingdom,  
 and Département de Chimie, École Normale Supérieure, 24 rue Lhomond, 75005 Paris, France

Received: September 18, 2003; In Final Form: December 18, 2003

We use the thread model for linear chains of interacting monomers and the “polymer reference interaction site model” formalism to determine the monomer–monomer pair correlation function  $h_{mm}(r)$  for dilute and semidilute polymer solutions, over a range of temperatures from very high (where the chains behave as self-avoiding walks) to below the  $\theta$  temperature, where phase separation sets in. An inversion procedure, based on the HNC integral equation, is used to extract the effective pair potential between “average” monomers on different chains. An accurate relation between  $h_{mm}(r)$ ,  $h_{cc}(r)$  (the pair correlation function between the polymer centers of mass (c.m.)), and the intramolecular form factors is then used to determine  $h_{cc}(r)$  and subsequently extract the effective c.m.–c.m. pair potential  $v_{cc}(r)$  by a similar inversion procedure.  $v_{cc}(r)$  depends on temperature and polymer concentration, and the predicted variations are in reasonable agreement with recent simulation data, except at very high temperatures and below the  $\theta$  temperature.

## I. Introduction

The statistical mechanics of dilute and semidilute solutions of interacting polymers may be greatly simplified by adopting a coarse-graining strategy for this complex many-body system, whereby the initial monomer or segment-level description is reduced to a “soft-colloid” representation involving only the centers of mass (c.m.) of the polymer coils. This is formally achieved by tracing out the individual monomer degrees of freedom for fixed positions of the c.m.’s of the polymers. This reduction procedure results in effective interactions between the c.m.’s, which are state dependent, since they are in fact *free* energies of the “fluid” of monomers, for each configuration of the c.m.’s of the  $N$  interacting coils. In the low concentration limit, this free energy reduces to a pairwise additive sum of effective potentials of mean force acting between the c.m.’s of overlapping polymers, which depend only on temperature. Such pair potentials were first considered by Flory and Krigbaum<sup>1</sup> and later put on a firmer basis by Grosberg et al.,<sup>2</sup> who showed that the effective pair potential between the c.m.’s of linear self-avoiding walk (SAW) polymers remains finite at full overlap in the scaling limit (where the number of segments  $L \rightarrow \infty$ ), and of the order of a few  $k_B T$ , reflecting the purely entropic origin of the effective interaction in the athermal SAW model. Quantitative estimates of the effective c.m. pair potential between two isolated SAW polymers were obtained by Monte Carlo (MC) simulations of on- and off-lattice models<sup>3–7</sup> and by renormalization group calculations.<sup>8</sup> These studies show that the zero concentration pair potential is purely repulsive and reasonably well represented by a Gaussian of amplitude  $\approx 2k_B T$  and width equal to the radius of gyration  $R_g$ .

The SAW model describes polymers in good solvent conditions. Poor solvent conditions may be modeled by adding a finite attractive interaction between monomers and lowering the temperature. MC simulations<sup>4,9</sup> show that the resulting effective c.m. pair potential becomes less repulsive as the temperature  $T$  is lowered and can become attractive in the vicinity of the  $\theta$  temperature.

When the polymer concentration is increased, three- and more-body effective interactions between the polymer c.m.’s come into play. These can also in principle be calculated by MC simulations of clusters of three or more polymers,<sup>10</sup> but this systematic procedure becomes rapidly untractable since the effective interactions depend on an increasing number of variables.

An alternative approach is to restrict the effective interactions between polymer c.m.’s at finite concentrations to a sum of pair potentials, the latter being determined by an inversion procedure of the c.m. pair distribution function based on integral equations for the pair structure of classical fluids.<sup>5–7,9</sup> The price to pay is that the resulting pair potentials now depend on polymer concentration, in addition to temperature. The variation with concentration is moderate but significant, in the case of the SAW model for polymers in good solvent conditions,<sup>5–7</sup> and becomes very strong for polymers in poor solvent conditions.<sup>9</sup>

Since the effective pair potentials are obtained by inverting c.m. pair correlation data from MC simulations, this strong variation with polymer concentration means that full monomer-level simulations must be carried out for each thermodynamic state of the polymer solution, thus partly defeating the purpose of the coarse-graining strategy.

It is hence important to explore numerically less-demanding theoretical methods for the determination of the required polymer pair correlation functions. One obvious candidate is the polymer reference interaction site model (PRISM) theory, which has proved very successful to determine the pair structure of interacting polymer solutions and melts.<sup>11</sup> PRISM grew out

<sup>†</sup> Part of the special issue “Hans C. Andersen Festschrift”.

\* Author to whom correspondence may be addressed. E-mail: Vincent.Krakoviack@ens-lyon.fr.

<sup>‡</sup> École Normale Supérieure de Lyon.

<sup>§</sup> University of Cambridge.

<sup>||</sup> École Normale Supérieure.

of the RISM integral equation of Chandler and Andersen<sup>12</sup> for the pair structure of simple molecular fluids. The theory includes intramolecular connectivity via the macromolecular form factor, and provides accurate monomer–monomer pair distribution functions,  $g_{mm}(r)$ . The c.m.–c.m. pair distribution function,  $g_{cc}(r)$ , which needs to be inverted to extract the effective c.m.–c.m. pair potential,  $v_{cc}(r)$ , can be derived from  $g_{mm}(r)$  by a simple, accurate relation which was established recently within the PRISM framework.<sup>13</sup>

This strategy, which is highly economical on computational resources, is explicitly carried out in this paper, on the basis of the Gaussian thread model for interacting polymers.<sup>14–17</sup> PRISM theory, in conjunction with an approximate closure relation, allows the monomer–monomer pair distribution function  $g_{mm}(r)$  to be calculated analytically or numerically depending on the expression for the polymer form factor. The c.m. pair distribution function is then extracted from  $g_{mm}(r)$  using the relation of ref 13 together with appropriate form factors, and  $v_{cc}(r)$  is finally obtained by hypernetted chain (HNC) inversion.<sup>5–7,9</sup> The variation of the effective pair potential with temperature and polymer concentration is then examined in detail and compared to the “exact” results extracted from MC simulations.<sup>5–7,9</sup>

## II. Polymer Model and PRISM Theory

We consider solutions of  $N$  linear polymers made up of  $L$  freely jointed monomers or segments of diameter  $d$  and spacing  $\sigma$ . Monomers belonging to the same or different chains are not allowed to overlap; i.e., they experience an infinite mutual repulsion for monomer–monomer distances  $r < d$ , and for  $r > d$ , they attract each other via a Yukawa interaction

$$v(r) = -\epsilon \frac{a}{r} e^{-r/a} \quad (1)$$

where  $\epsilon > 0$  is the energy scale and  $a$  the range of the monomer–monomer attraction.<sup>15,16</sup> The relevant thermodynamic variables are the temperature  $T$  (as usual, we define  $\beta = (k_B T)^{-1}$ ) and the polymer concentration  $\rho$  (number of polymer coils per unit volume); the corresponding monomer density is  $\rho_m = \rho L$ . As usual, the spatial extension of the chain will be characterized by its radius of gyration  $R_g$ , and the polymer overlap concentration, at which different chains start to overlap, is defined as  $\rho^* = ((4/3)\pi R_g^3)^{-1}$ . In this model of polymer solutions, the attractive interaction (1) represents solvent-mediated monomer–monomer interactions in an effective way. Then, with respect to intermolecular interactions, large  $T$  values correspond to good solvent conditions, while lower  $T$  values mimic poor solvent conditions.

PRISM theory assumes all monomers to be equivalent regardless of their position along the polymer chain. Its aim is to calculate the site-averaged pair distribution function  $g_{mm}(r)$  of monomers on different chains. To this end, one introduces the pair correlation function,  $h_{mm}(r) = g_{mm}(r) - 1$ , the direct correlation function  $c_{mm}(r)$ , and their Fourier transforms, respectively,  $\hat{h}_{mm}(q)$  and  $\hat{c}_{mm}(q)$ , which are related by the following generalization of the Ornstein–Zernike (OZ) equation<sup>11</sup>

$$\hat{h}_{mm}(q) = \hat{\omega}_{mm}(q) \hat{c}_{mm}(q) (\hat{\omega}_{mm}(q) + \rho_m \hat{h}_{mm}(q)) \quad (2)$$

where  $\hat{\omega}_{mm}(q)$  is the form factor of the polymer chains. In the following, it will be convenient to introduce the auxiliary quantities  $\hat{\Omega}_{mm}(q) = \hat{\omega}_{mm}(q)/L$  (hence,  $\hat{\Omega}_{mm}(q = 0) = 1$ ) and  $\hat{C}_{mm}(q) = L^2 \hat{c}_{mm}(q)$ , such that eq 2 may be rewritten as

$$\hat{h}_{mm}(q) = \hat{\Omega}_{mm}(q) \hat{C}_{mm}(q) (\hat{\Omega}_{mm}(q) + \rho \hat{h}_{mm}(q)) \quad (3)$$

The OZ equation, eq 3, must be supplemented by a closure relation for  $\hat{C}_{mm}(q)$  as well as by a prescription for  $\hat{\Omega}_{mm}(q)$ . While self-consistent schemes exist to compute the latter as a function of temperature and density, they are quite complex to implement.<sup>11</sup> In the present work, we will make the simplifying assumption that the polymers obey Gaussian statistics. This approximation, which is in principle only valid in the melt or close to the  $\theta$  temperature, is mainly needed for technical reasons due to the lack of analytical results for non-Gaussian polymers. Thus, the form factor  $\hat{\Omega}_{mm}(q)$  is given by the well-known Debye expression for ideal chains in the continuum limit, namely<sup>18</sup>

$$\hat{\Omega}_{mm}(q) = \frac{2}{x^4} (e^{-x^2} - 1 + x^2) \quad x = qR_g \quad (4)$$

Replacing this exact form by its simple Padé approximant

$$\hat{\Omega}_{mm}(q) = \frac{1}{1 + x^2/2} \quad x = qR_g \quad (5)$$

allows analytic results to be obtained within the thread limit,<sup>14–16</sup> but we will see in the following that it can lead to significant problems in the present context.

In this work, we are interested in a mesoscopic level of description of polymer systems. For simplicity, it is thus useful to get rid of the microscopic details of the polymer model. A way of doing this in the PRISM framework is by taking the so-called thread limit. In the case of excluded-volume interactions only, it is defined by letting  $d$  and  $\sigma$  go to zero and  $L$  to infinity, keeping the ratio  $\Gamma = \sigma/d$ ,  $R_g$ , and  $\rho/\rho^* = (4/3)\pi\rho R_g^3$  constant.<sup>14–16,19,20</sup> In refs 15 and 16, the attractive part of the monomer–monomer interaction potential was left untouched when taking the thread limit. However, for simple polymers, it turns out that the range of this attractive tail scales with the monomer size. Thus for this work, it seemed physically appropriate to supplement the previous limiting process with the limit of a vanishing range of the attractive potential, namely,  $a \rightarrow 0$ , keeping the ratio  $\Delta = a/\sigma$  constant. This can be interpreted as a special limit of the theory of refs 15 and 16 as shown in Appendix A.

To escape the trivial case of noninteracting polymers, the thread limit requires a proper formulation of the closures of the PRISM–OZ eq 3 as well. In this work, we have applied the so-called RMPY/HTA closure, which has been found to be the most satisfactory in earlier work.<sup>15,16,21</sup> The details are given in Appendix A, and we only quote here the equations relevant to our calculation. The monomer–monomer correlations are thus given by

$$\hat{h}_{mm}(q) = \frac{\tilde{c} R_g^3 \hat{\Omega}_{mm}(q)^2}{1 - \rho \tilde{c} R_g^3 \hat{\Omega}_{mm}(q)} \quad (6)$$

with

$$\tilde{c} = \tilde{c}_0 \left(1 - \frac{\Theta}{T}\right) \quad (7)$$

where  $\Theta$  is the  $\theta$  temperature of the polymer model.  $\tilde{c}_0$ , which depends on  $\rho R_g^3$  only, is obtained by imposing that, in the presence of excluded-volume interactions only (i.e., for infinite temperature),  $h_{mm}$  obeys the hard-core condition,  $h_{mm}(r = 0) = -1$ . It is plotted for both chain form factors, eqs 4 and 5, in Figure 1.

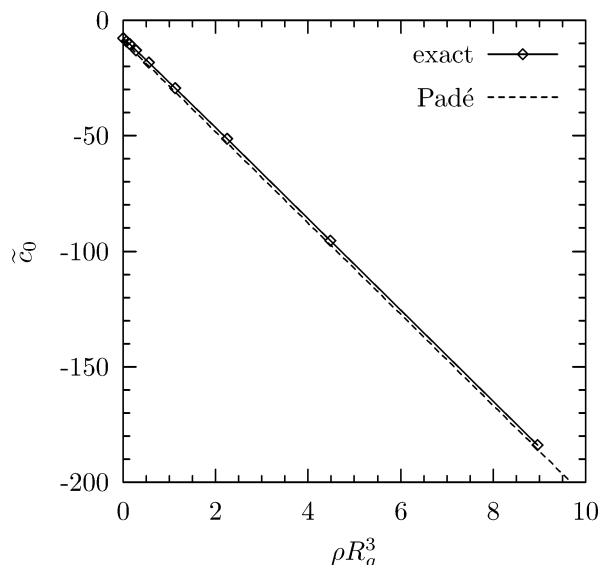


**Figure 1.** Density dependence of the direct correlation function  $\tilde{c}_0$ , in the presence of excluded-volume interactions only. For the exact form factor (eq 4),  $\tilde{c}_0$  has to be numerically determined, while for the approximation (eq 5), the analytic result (A2) is plotted.

With the above monomer pair correlation functions, effective pair potentials between polymer chains may now be determined. We first consider in the next section the situation where the interaction site for the effective interaction between polymer coils is chosen to be a monomer; subsequently, effective interactions between polymer c.m.'s are discussed in section IV.

### III. Effective Interaction between Monomers

Starting from the original polymer system, the choice of the effective coordinates used to specify the position of each polymer coil, and relative to which the coarse-graining procedure is performed, is largely arbitrary. Most of the time, the center of mass is considered, but it has sometimes been suggested to use specific monomers, such as the midpoint or the endpoints, as in refs 6, 7, and 22. This is a very natural choice for star polymers as well, where the star center provides an obvious reference point.<sup>23</sup> In this section, we thus attempt to build such a monomer–monomer (or site–site) effective interaction.

In the present PRISM-based approach, by construction, no distinction is made between the different monomers on a chain. However, one can build an effective monomer–monomer interaction based on the concept of an average monomer.<sup>24</sup> The idea goes as follows. On each chain, a random monomer is tagged, and a coarse-grained polymer–polymer interaction is computed by tracing out, for fixed (spatial) positions of the tagged monomers, all the other monomer degrees of freedom. Averaging this free energy over the random locations of the tagged monomers on their chains then leads to a quantity that can be given the meaning of an effective interaction between average monomers.

In practice, an effective pair potential  $v_{aa}(r)$  may be extracted by an inversion procedure, based on integral equations for the pair structure of simple fluids.<sup>25</sup> For this purpose, we consider a fluid of average monomers, of density  $\rho$  (each polymer chain is originally associated with a single tagged interaction site), the pair correlations of which are characterized by  $h_{aa}(r) \equiv h_{mm}(r)$ , where  $h_{mm}(r)$  is the monomer-averaged correlation function determined in the previous section.<sup>26</sup> A direct correlation function  $c_{aa}(r)$  may be extracted from  $h_{aa}(r)$  via the OZ

relation for simple (atomic) fluids which in Fourier space reads

$$\hat{h}_{aa}(q) = \hat{c}_{aa}(q)(1 + \rho \hat{h}_{aa}(q)) \quad (8)$$

The effective interaction potential may finally be determined using one of the standard closures for simple fluids. Since the effective interactions are expected to be relatively weak (in particular, they contain no hard-core repulsion), we follow earlier work<sup>5–7,9</sup> and adopt the very accurate HNC closure, which leads to the following expression for  $v_{aa}(r)$

$$\beta v_{aa}(r) = h_{aa}(r) - c_{aa}(r) - \ln(1 + h_{aa}(r)) \quad (9)$$

With this closure, a fully analytic expression for  $\beta v_{aa}(r)$  can be obtained if the approximate expression (5) for the chain form factor is used. Details are given in Appendix B.

We first consider the case of excluded-volume interactions only, i.e.,  $\tilde{c} = \tilde{c}_0$ . The analytic  $\beta v_{aa}(r)$  is plotted in Figure 2 for various polymer densities. It diverges at zero separation, and when the density increases, this divergence manifests itself at shorter distances and becomes steeper. At the same time, the repulsive tail of the potential becomes longer ranged, as can be clearly seen on the plot of  $4\pi(r/R_g)^2\beta v_{aa}(r)$ , a quantity playing a crucial role for the calculation of the thermodynamic properties of fluid systems characterized by similar “soft” interaction potentials.<sup>27</sup> These results are in good qualitative agreement with the simulation data of Bolhuis and Louis for midpoint and endpoint effective pair potentials.<sup>7</sup>

Recently, much attention has been devoted to the development of analytic expressions for effective pair potentials between the centers of star polymers in solution.<sup>23</sup> Since a linear polymer, seen from one of its endpoints or from its midpoint, can be identified with a one- or two-arm star, respectively, it is interesting to compare those calculations with the present theory.

Since, according to eq A3,  $1 + h_{mm}(r)$  vanishes linearly for  $r \rightarrow 0$ ,  $\beta v_{aa}(r)$  diverges as  $-\ln(r/R_g)$ . Such a weak, logarithmic divergence is present in the star polymer models, where it has been derived using scaling arguments, but the prefactor, which should be given by the two-arm result in the limit of very long chains where end effects are expected to be negligible, appears overestimated by the present theory compared to scaling arguments (which predict a prefactor equal to  $5f^{3/2}/18$  for a star with  $f$  arms) and renormalization group results.<sup>28</sup> This quantitative disagreement is not surprising, since the present calculation relies on the use of Gaussian form factors in good solvent conditions. However, a similar calculation done with an approximate form factor reproducing the correct asymptotic behavior of  $\hat{\Omega}_{mm}(q)$  in good solvent conditions still does not provide the correct value, and this failure was in fact argued to be inherent to the thread PRISM approach.<sup>19</sup>

For large distances,  $\beta v_{aa}(r)$  asymptotically takes a Yukawa form<sup>29</sup>

$$\beta v_{aa}(r) \propto \frac{e^{-r/\xi^+}}{r/R_g} \quad (10)$$

Such long-range behavior was postulated for star polymers, on the basis of the blob picture of the star inner structure. However, because the blob picture breaks down for small  $f$ , it was advocated that this asymptotic behavior should not be valid for small functionalities,  $f \lesssim 10$ , and should be replaced by a Gaussian tail, by analogy with the behavior of the effective pair potential between chain c.m.'s.<sup>22</sup> The present calculation does not appear to support this choice.

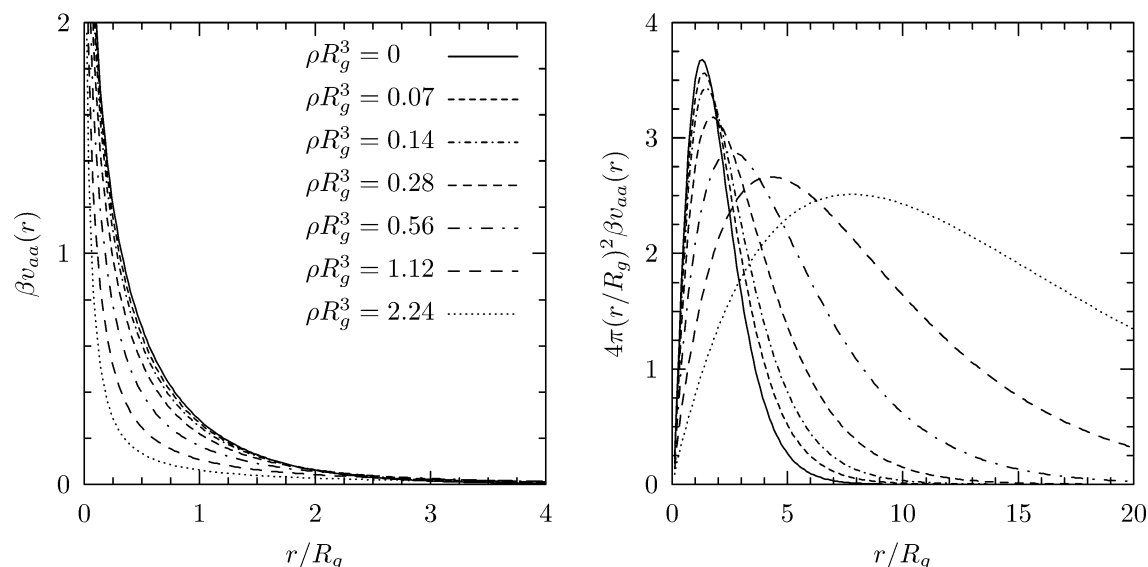


**Figure 2.** Effective pair potentials between average monomers (left-hand frame), obtained with the approximate polymer form factor (eq 5), at various reduced densities  $\rho R_g^3$ , in the presence of excluded-volume interactions only. The right-hand frame shows the potentials multiplied by  $4\pi(r/R_g)^2$ .

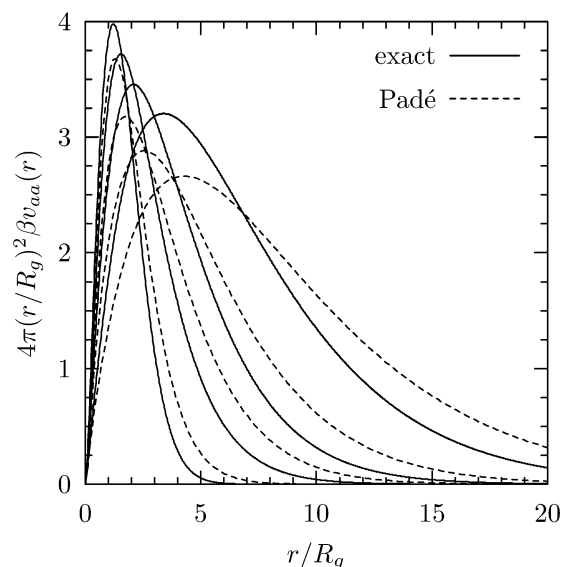


**Figure 3.** Comparison of the effective pair potentials between average monomers (multiplied by  $4\pi(r/R_g)^2$ ) obtained with the exact and approximate polymer form factors, eqs 4 and 5, respectively, at various densities, in the presence of excluded-volume interactions only. From left to right:  $\rho R_g^3 = 0, 0.28, 0.56, 1.12$ .

Finally, and maybe more importantly, the present calculation reveals that  $\beta v_{aa}(r)$  changes significantly with density. For instance, the range of the asymptotic Yukawa tail more than doubles between  $\rho/\rho^* = 0$  and  $\rho/\rho^* = 1$ . If such a behavior also applies to star polymers, it could have a major impact on the calculation of the thermodynamic properties of these systems, in particular on their phase diagrams.

In Figure 3, the numerically determined  $\beta v_{aa}(r)$  for the exact Debye form factor (4) is compared to the analytic result obtained with the Padé approximant (5) at various polymer densities. A thorough analysis shows that the differences between both are only quantitative. Both share the same  $-\ln(r/R_g)$  divergence for small separations, and both display an asymptotic Yukawa tail, which is of shorter range when eq 4 is used.

We now turn to the effect of the attractive monomer–monomer interaction with changing temperature. In Figure 4,

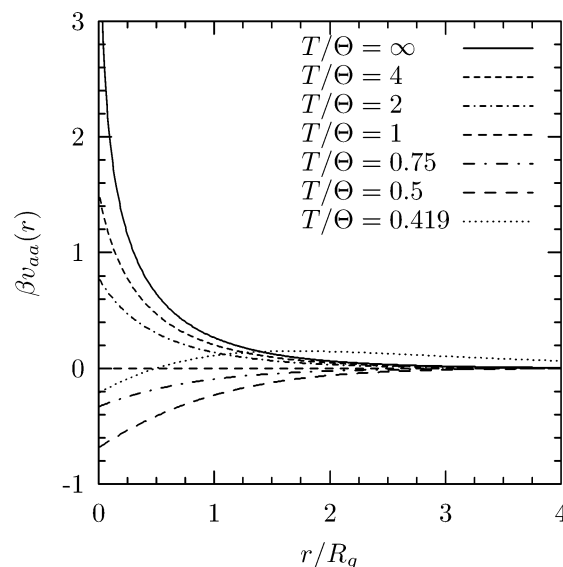


**Figure 4.** Effective pair potentials between average monomers, obtained with the approximate polymer form factor (eq 5), at various temperatures, for the reduced density  $\rho R_g^3 = 0.07$ .

the analytic  $\beta v_{aa}(r)$  calculated with the approximate chain form factor (5) is plotted at density  $\rho R_g^3 = 0.07$  for various values of the temperature. Similar results are obtained at all densities and with the exact Debye form factor as well. The effective potential is seen to become less repulsive when the temperature is decreased from  $\infty$  to  $\Theta$ ; it vanishes identically at  $\Theta$  and grows more and more attractive if the temperature is further decreased. This trend reverts when the “spinodal” line is approached, leading to nonmonotonic, mostly repulsive effective potentials of increasing range.

But a word of caution is needed here. Indeed, as shown in Appendix A, at all finite temperatures, the hard-core condition  $h_{mm}(r=0) = -1$  is no longer obeyed. Thus, the effective pair potential between average monomers does not diverge at full overlap as it should if this condition was consistently enforced at all state points. This might not be so important since, as it has already been mentioned, the product  $4\pi(r/R_g)^2 \beta v_{aa}(r)$  is in general more relevant than the potential itself, and in this



quantity the short-range details of the potential are strongly reduced by the vanishing prefactor. Another source of concern is that it is not known to what extent the results obtained below  $\Theta$  when approaching the “spinodal” line are physically meaningful since the corresponding remnant of a binodal line, which would properly identify the domain of existence of the low-density phase, is not known in the present theory.<sup>30</sup> For these reasons, the present results are only given for reference and would need to be validated both by implementing alternative integral equation schemes or by investigating  $\beta v_{aa}(r)$  as a function of temperature by molecular simulation.

To summarize, we have shown in this section that integral equation theories for macromolecular systems, like the present thread PRISM theory, could be useful tools to compute monomer-based effective interaction potentials between polymers. At least in the case of excluded-volume interactions only, they lead to very reasonable predictions for the effective interactions between average monomers on polymer chains, compared to the presently available simulation and theoretical results.

But the concept of an average monomer, which is needed in the present theory because, at variance with star polymers, there is no obvious choice of a reference monomer, is rather artificial and in practice conceals significant technical difficulties. Indeed, this concept has a simple meaning only in the limit of very long chains, where all monomers can be considered as equivalent. In ref 7, the effective interactions between central monomers and between end monomers have been found to differ considerably, showing that strong finite length effects should be expected on effective interactions between average monomers. Thus, for a better control of these finite size effects, an alternative approach seems desirable, and it has been found that considering effective interactions between polymer c.m.’s is appropriate in this respect.<sup>3–7</sup>

#### IV. Effective Interaction between Centers of Mass

As has been shown in recent Monte Carlo studies,<sup>5–7,9</sup> an effective pair potential  $v_{cc}(r)$  between the c.m.’s of polymer chains may be extracted by an inversion procedure analogous to the one described in the previous section. To that purpose, one considers a simple fluid of density  $\rho$ , the pair correlations of which are characterized by  $h_{cc}(r)$ , the c.m. correlation function of the polymer system. The corresponding direct correlation function will be denoted  $c_{cc}(r)$ .

The c.m. correlation function  $h_{cc}(r)$  is easily accessible in MC simulations for any polymer concentration<sup>5–7,9</sup> but cannot be calculated directly from the original PRISM integral equation. However an approximate relation between  $\hat{h}_{mm}$  and  $\hat{h}_{cc}$  was established in ref 13, which reads

$$\hat{h}_{cc}(q) \approx \left( \frac{\hat{\Omega}_{cm}(q)}{\hat{\Omega}_{mm}(q)} \right)^2 \hat{h}_{mm}(q) \quad (11)$$

where  $\hat{\Omega}_{mm}(q)$  is the previously discussed intramolecular monomer–monomer form factor and  $\hat{\Omega}_{cm}(q)$  is the c.m.–monomer form factor (normalized such that  $\hat{\Omega}_{cm}(q=0) = 1$ ). This relation was shown to be quite accurate by comparing the resulting  $\hat{h}_{cc}(q)$ , or the corresponding c.m. structure factor  $S_{cc}(q) = 1 + \rho \hat{h}_{cc}(q)$ , to MC simulation data. To complete the results of ref 13, where only good solvent conditions were explored, and to illustrate the quality of the predictions of eq 11 for  $S_{cc}(q)$ , simulation results obtained for a lattice model slightly below its  $\theta$  temperature are reported in Figure 5.

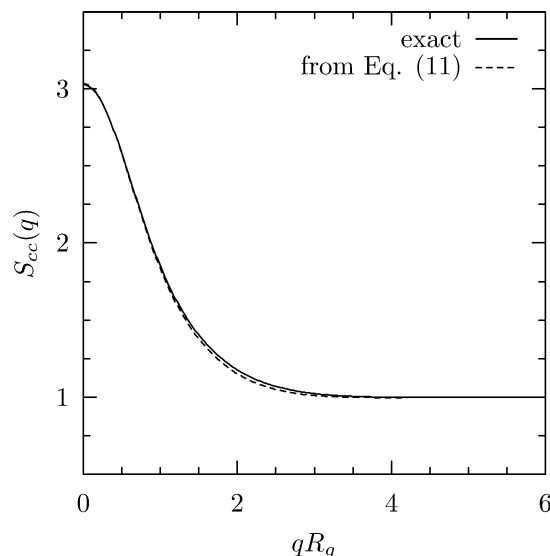


**Figure 5.** c.m. structure factor  $S_{cc}(q)$  for  $L = 500$  SAW polymers with monomer nearest-neighbor interaction  $\epsilon$  on a simple cubic lattice, at  $\beta\epsilon = 0.3$  and  $\rho R_g^3 \approx 0.04$ . The “exact” structure factor from MC simulations is compared to the prediction of the approximation (eq 11) using the “exact” monomer correlation function and form factors.

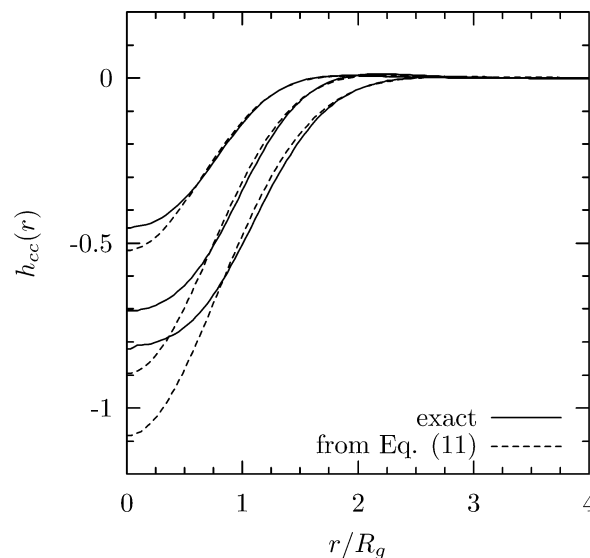


**Figure 6.** c.m. pair correlation functions  $h_{cc}(r)$  for  $L = 500$  SAW polymers on a simple cubic lattice. From bottom to top,  $\rho R_g^3 \approx 0.07, 0.27, 1.10$ . The “exact” pair correlation functions are compared to the predictions of the approximation (11) using the “exact” monomer correlation functions and form factors.

However, to use eq 9, we explicitly need the pair correlation function  $h_{cc}(r)$ ; i.e., we have to formulate the predictions of eq 11 in real space and not in reciprocal space. In Figure 6, we plot the simulation results of ref 13 accordingly. The agreement between the “exact”  $h_{cc}(r)$  and its approximation computed from eq 11, using the “exact” monomer correlation function and form factors, is seen to be reasonably good, except at short distances where the results of the approximation lie well below the “exact” simulation data and can even become smaller than  $-1$  at low densities, which is unphysical. Consequences of this underestimation of  $h_{cc}(r)$  at full overlap, which is found under the conditions of Figure 5 as well and appears to be systematic, are discussed below.

As mentioned in section II, since there are no known analytic expressions for the two form factors appearing in eq 11 for interacting polymers, we are led to use the expressions valid

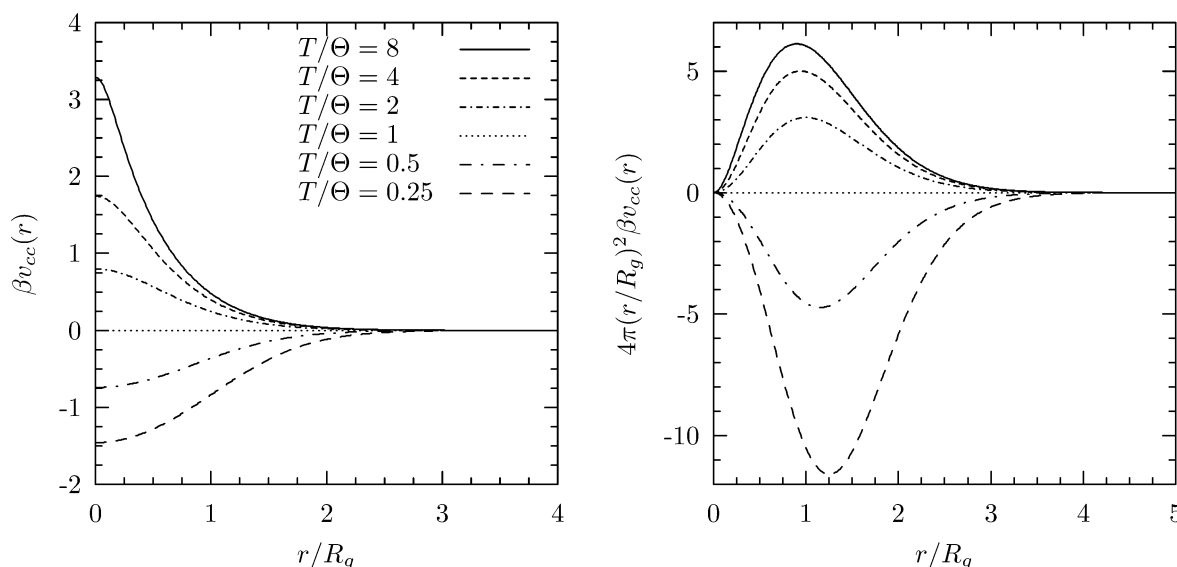


**Figure 7.** Zero-density effective pair potentials between c.m.'s (left-hand frame), for various values of the temperature ratio  $T/\Theta$ . The right-hand frame shows the potentials multiplied by  $4\pi(r/R_g)^2$ .

for Gaussian polymer coils in the scaling limit,<sup>31</sup> i.e., eq 4 and

$$\hat{\Omega}_{\text{cm}}(q) = \frac{(\pi)^{1/2}}{x} e^{-x^2/12} \text{erf}\left(\frac{x}{2}\right) \quad x = qR_g \quad (12)$$

where erf denotes the error function. In ref 13, it was shown that they yield qualitatively correct results for the calculation of  $\hat{h}_{\text{cc}}(q)$ , even in the good solvent regime.

The importance of using exact results is best seen when the high-density limit of  $\hat{h}_{\text{cc}}(q)$  for  $T > \Theta$  is considered, which follows from eq 6

$$\lim_{\rho \rightarrow \infty} \rho \hat{h}_{\text{cc}}(q) = - \frac{\hat{\Omega}_{\text{cm}}(q)^2}{\hat{\Omega}_{\text{mm}}(q)} \quad (13)$$

Indeed, while this ratio is always larger than  $-1$  if the exact form factors 4 and 12 are combined, it shows a region at small  $q$  where it is smaller than  $-1$  if the approximation 5 is used. In the latter case, spurious singularities are thus encountered when eq 8 is applied to compute  $\hat{c}_{\text{cc}}(q)$  at high densities.

In this high density regime, an expression for the potential of mean force between the c.m.'s of polymers in the melt has been derived by Guenza, on the basis of the same thread PRISM theory as the one used here, in the case of excluded-volume interactions only.<sup>32</sup> Both approaches share similarities, in particular the fact that, to first order, the potential of mean force vanishes proportionally to  $1/\rho$ . However, since many aspects of these theories differ and since we are interested in the effective potential and not the potential of mean force, a detailed comparison was not attempted.

The outline of the present computation is thus the following. First, the thread PRISM theory developed in section II is used to obtain  $h_{\text{mm}}(r)$ . Then  $h_{\text{cc}}(r)$  is derived by applying eq 11 with form factors 4 and 12 and is eventually inverted using eqs 8 and 9 with index c instead of a) to obtain  $\beta v_{\text{cc}}(r)$ .

We first consider the zero density limit. When  $\rho \equiv 0$ , the effective pair potential is simply the potential of mean force, i.e.,  $\beta v_{\text{cc}}(r) = -\ln(1 + h_{\text{cc}}(r))$ . Combining eqs 6 (with  $\rho = 0$ ) and 11, one finds

$$\beta v_{\text{cc}}(r) = -\ln(1 + \tilde{c}R_g^3 \Omega_{\text{cm}} * \Omega_{\text{cm}}(r)) \quad (14)$$

where an asterisk denotes a space convolution. Results for  $\beta v_{\text{cc}}(r)$  and  $4\pi(r/R_g)^2 \beta v_{\text{cc}}(r)$  are shown in Figure 7 for several temperatures. Above  $\Theta$ ,  $\beta v_{\text{cc}}(r)$  has a roughly Gaussian shape, with an amplitude that decreases with temperature. The potential vanishes identically for  $T = \Theta$  and becomes purely attractive below, retaining a roughly Gaussian shape with a negative amplitude increasing in absolute value when  $T$  is decreased. These trends are globally in agreement with the behavior found in MC simulations,<sup>4,9</sup> but quantitative differences are visible.

In the good solvent regime, for temperatures above approximately  $11\Theta$ , it is impossible to compute  $\beta v_{\text{cc}}(r)$ . This is due to the theory producing unphysical c.m. pair distribution functions, which are negative in the vicinity of  $r = 0$ . Moreover, approaching this existence limit from below, the value of  $\beta v_{\text{cc}}(r)$  at full overlap is found to diverge, corresponding to the fact that  $h_{\text{cc}}(r = 0)$  goes to  $-1$ . This behavior is at odds with all available simulation data<sup>3-7,9</sup> and other theoretical approaches,<sup>2,8</sup> showing that in good solvent the amplitude of the potential of mean force is always finite and has a maximum of about  $2k_B T$ , a value reached for  $T \approx 5\Theta$  in the present theory. This deficiency, which manifests itself throughout the high- $T$ , low- $\rho$  domain, is an obvious consequence of the underestimation of  $h_{\text{cc}}(r)$  at full overlap, as illustrated in Figure 6. While the exact  $h_{\text{cc}}(r = 0)$  saturates at a value strictly greater than  $-1$  in the limit of infinite temperature, it is predicted by the present theory to go to  $-1.1$  in the same limit. At this point, it is worth insisting on the fact that this problem appears to be associated with the use of eq 11 and is totally unrelated to the use of Gaussian chain form factors to model good solvent conditions.

Around and below  $\Theta$ , a more complex  $r$  dependence of  $\beta v_{\text{cc}}(r)$  was found in the simulations of refs 4 and 9, the potential globally growing more and more negative, as found here, but retaining a repulsive component at short distances, while it is found strictly monotonic in the present calculation. These two types of variations were also found in various theoretical approaches based on mean-field ideas,<sup>1,33-36</sup> and in fact, it is not clear what the generic behavior of  $\beta v_{\text{cc}}(r)$  is in poor solvents. The available simulation data were indeed obtained for rather short chains, for which, on the scale of  $R_g$ , the monomer hard cores are not of negligible size. This could result in the observed short-range repulsive contribution to  $\beta v_{\text{cc}}(r)$ , which would then be a finite size effect disappearing for longer chains.<sup>37</sup>

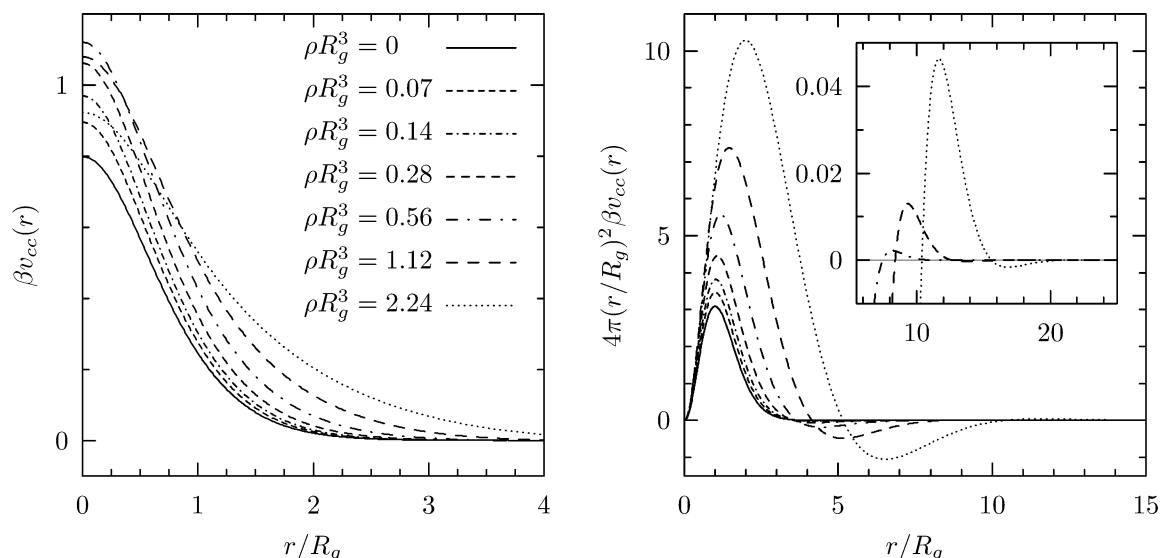


**Figure 8.** Effective pair potentials between c.m.'s (left-hand frame), at temperature  $T = 2\Theta$ , for various values of the reduced density  $\rho R_g^3$ . The right-hand frame shows the potentials multiplied by  $4\pi(r/R_g)^2$ , and the insert shows an enlargement of this function for large  $r/R_g$ .

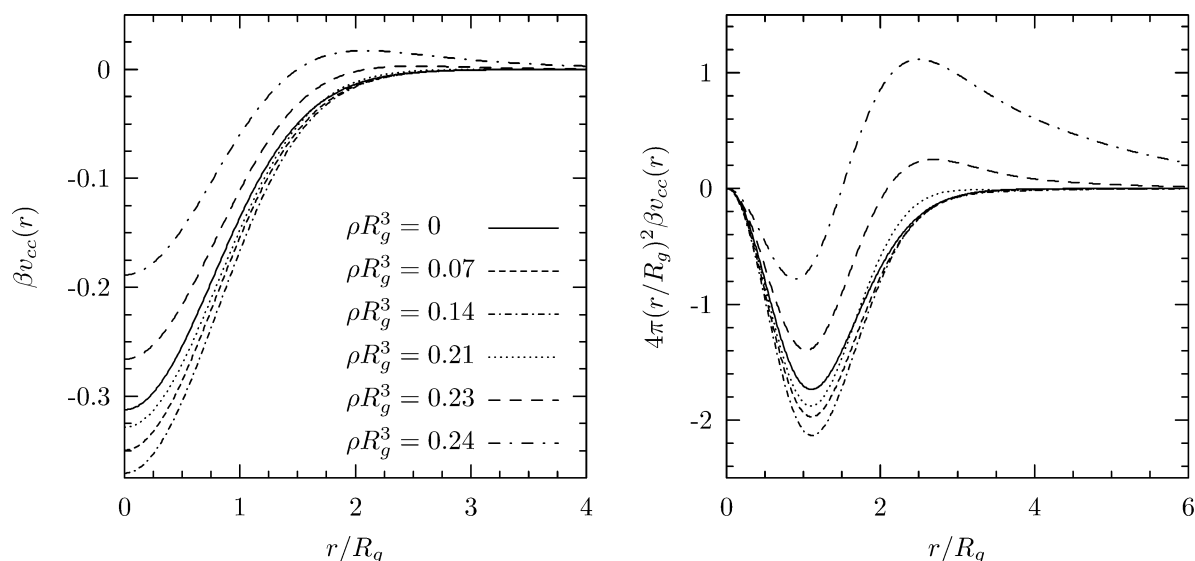


**Figure 9.** Effective pair potentials between c.m.'s (left-hand frame), at temperature  $T = 0.75\Theta$ , for various values of the reduced density  $\rho R_g^3$ . The right-hand frame shows the potentials multiplied by  $4\pi(r/R_g)^2$ .

By comparison with mean-field theories, difficulties can in fact be anticipated with the present theory in the low-temperature domain. Indeed, in the zero density limit, following eq 14,  $\beta v_{cc}(r)$  is a simple function of the overlap between the monomer distributions around the centers of mass of two coils at distance  $r$ . However, mean-field theories built exclusively on this two-polymer overlap are known to take into account only two-body effective monomer–monomer interactions. This is for instance the case of the theory of Flory and Krigbaum,<sup>1,34</sup> which can be recovered in a thread PRISM version by linearizing eq 14. Such approaches are valid in good solvent conditions since then pair interactions actually dominate, but they fail in  $\Theta$  and poor solvents, where inclusion of higher order interactions is required. By analogy, this raises questions on the applicability of the present theory in the latter domain as well.

We now turn to the density dependence of the effective potentials derived within the present theory. Effective potentials obtained for various densities at  $T = 2\Theta$  are plotted in Figure 8. These results are typical of good solvent conditions. Starting from  $\rho R_g^3 = 0$ , where the potential is purely repulsive and nearly Gaussian,  $v_{cc}(r)$  first increases in amplitude and in range

with  $\rho R_g^3$ , then at a density which increases when the temperature approaches  $\Theta$  from above, the trend changes. The repulsion at full overlap decreases as  $\rho R_g^3$  is further increased, while the range of the effective potential still increases. In addition, with increasing  $\rho R_g^3$ , a damped oscillatory tail, which is more clearly seen on plots of  $4\pi(r/R_g)^2 \beta v_{cc}(r)$ , progressively develops when the distance between the c.m.'s of two coils greatly exceeds  $R_g$ . All these trends are consistent with the simulation data of refs 5–7 and 9. The only qualitative difference is in the tail of the potential, which, within the resolution of the simulations, appears to be purely attractive. The results of the present theory suggest that to unveil a possible oscillatory behavior, simulations of much larger bulk systems with very high statistical accuracy would be required to characterize the potential beyond its first minimum.

Despite the various concerns discussed above about the applicability of the present theory around and below the  $\theta$  temperature (lack of more-than-two-body effective monomer–monomer interactions, incomplete characterization of the domain of existence of the low-density phase),<sup>30</sup> we present the

corresponding results for completeness. When  $T = \Theta$ , the effective c.m. potential is found to vanish identically at all densities. Typical results for the poor solvent domain, obtained for various densities at  $T = 0.75\Theta$ , are plotted in Figure 9. Starting from  $\rho R_g^3 = 0$ , where the potential is negative and nearly Gaussian,  $v_{cc}(r)$  is first found to become more negative with increasing  $\rho R_g^3$ , while roughly retaining its shape. Then, upon approaching the “spinodal” instability line, at a density which increases when the temperature approaches  $\Theta$  from below, the value of the potential at full overlap starts to grow with  $\rho R_g^3$  and a repulsive tail progressively develops. These tendencies are not corroborated by the presently available simulation data.

## V. Discussion and Conclusion

We have developed an integral equation approach to the computation of effective interactions between polymers in solution. It is based on the thread limit of the PRISM theory, which is used directly for the calculation of effective interactions between average monomers and in association with an approximate expression for the c.m. pair distribution function, derived within the PRISM formalism as well, for the calculation of c.m.–c.m. effective potentials.

In the case of the effective interactions between average monomers, the predictions of the theory for polymers with excluded-volume interactions only are in good qualitative agreement with the available simulation data. Moreover, we have shown that the theory lends itself to fully analytic calculations and compares rather favorably with other analytic theories such as those developed for star polymers.

The effective c.m.–c.m. interaction potentials derived from the present theory exhibit many of the trends observed in MC simulations. The agreement with the latter is very satisfactory at intermediate temperature under good solvent conditions, i.e.,  $T > \Theta$ . The theory indeed reproduces nontrivial features such as the nonmonotonic variation of the value of the potential at full overlap and the development of a long-range tail when the density increases. This agreement deteriorates at very high temperature, in particular for  $\beta = 0$  (SAW model), and around and below the  $\theta$  temperature.

Since the HNC closure used to compute the effective pair potential is exact for all practical purposes, when applied to “soft-core” systems that exhibit essentially “mean-field fluid” behavior,<sup>27</sup> the observed discrepancies must be traced back to the other approximations made in the theory, namely, the RMPY/HTA closure used to compute  $h_{mm}(r)$  in the thread limit, the use of form factors  $\hat{\Omega}_{mm}(q)$  and  $\hat{\Omega}_{cm}(q)$  valid for ideal rather than interacting chains, and eq 11 relating  $\hat{h}_{cc}(q)$  to  $\hat{h}_{mm}(q)$ . Simulation data tend to show that the use of eq 11 is the main cause of the breakdown of the theory at very high temperature, while there are indications that the present use of the RMPY/HTA closure in the low-temperature regime is not justified. In the present state of the theory, the use of ideal chain form factors is in fact not found to be a critical approximation.

In conclusion, we have proposed a first step toward an integral equation theory of effective pair potentials between macromolecules in solution, which could bypass costly simulations for the determination of the c.m. pair correlation function. The results appear very encouraging since, while only the simplest ingredients have been combined in the present theory and there is clearly room for improvement, it is already found to be able to capture various nontrivial behaviors observed in recent simulations. It appears thus that integral equation theories could

be in the future a valuable tool for the development of coarse-grained descriptions of complex polymeric systems.

## Appendix A: Thread PRISM Calculation

In this Appendix, we present our calculation of the monomer pair correlation function based on PRISM theory in the thread limit. It is inspired by the work of Chatterjee and Schweizer<sup>15,16</sup> (see also ref 17 for a related approach), a special asymptotic regime of which is obtained. We start with eq 3, involving quantities that all remain finite in the thread limit as defined in section II. The case of excluded-volume interactions only is considered first and then used as a reference system to include attractive interactions between the monomers in the closure relations.

### 1. Reference System: Excluded-Volume Interactions.

Considering first the excluded-volume interaction only, a Percus–Yevick (PY)-like closure is used, in which  $C_{mm}(r) = \tilde{c}_0 R_g^3 \delta(\mathbf{r})$  ( $R_g^3$  is introduced here to make  $\tilde{c}_0$  dimensionless) or equivalently in Fourier space

$$\hat{C}_{mm}(q) = \tilde{c}_0 R_g^3 \quad (A1)$$

This singular  $C_{mm}(r)$  is required to account for the effect of excluded volume on intermolecular correlations in the limit of vanishing size of the hard core of the monomers in the thread limit.

The PRISM-OZ relation (eq 3) then leads to eq 6, with  $\tilde{c} = \tilde{c}_0$ , and the value of  $\tilde{c}_0$  is determined by enforcing the hard-core condition  $h_{mm}(r=0) = -1$ .

In general, all the calculations have to be performed numerically. This is the case in the present work when  $\hat{\Omega}_{mm}(q)$  is chosen to be the Debye function (eq 4). However, fully analytic results can be obtained if the usual Padé approximant of this function, eq 5, is used. Then, one finds

$$\tilde{c}_0 = -2\pi(2)^{1/2} - 2\pi^2 \rho R_g^3 \quad (A2)$$

and

$$h_{mm}(r) = \frac{1}{2\pi \rho R_g^3} \frac{e^{-r/\xi_\rho} - e^{-r/\xi_c}}{r/R_g} \quad (A3)$$

where  $\xi_c = R_g/(2)^{1/2}$  and  $\xi_\rho = R_g/((2)^{1/2} + 2\pi \rho R_g^3)$ .

**2. Including an Attractive Tail.** We now introduce the attractive interaction between the monomers, which, for convenience, is taken of the Yukawa form (eq 1). In ref 15, various closures of the PRISM-OZ equation have been studied in the thread limit, for chains with monomers interacting through a hard core and an attractive tail. Here, we consider the reference molecular Percus–Yevick/high-temperature approximation (RMPY/HTA),<sup>15,16,21</sup> which has been found to be the most satisfactory in this earlier work. With the present notations, it reads

$$C_{mm}(r) = C_{ref}(r) - \beta V(r) g_{ref}(r) \quad (A4)$$

where a renormalized attractive potential  $V(r) = L^2 v(r)$  was introduced.  $C_{ref}(r)$  and  $g_{ref}(r)$  are, respectively, the renormalized monomer direct correlation function and the monomer pair distribution function of the reference system, the calculation of which is explained above.

As mentioned in section II on physical grounds, we supplement the previously applied limiting process with the limit of a vanishing range of the attractive potential, namely,  $a \rightarrow 0$ , keeping the ratio  $\Delta = a/\sigma$  constant. To take this supplementary



limit in the RMPY/HTA closure, we need to evaluate  $\lim_{a \rightarrow 0} \beta V(r) g_{\text{ref}}(r)$ . We assume that  $g_{\text{ref}}(r)$  satisfies the hard-core condition,  $g_{\text{ref}}(0) = 0$ , and has a finite slope at the origin. This hypothesis holds both for the analytic result, eq A3, and when the exact Debye form factor is used instead of its Padé approximant (see below). Then we can write the Taylor expansion

$$g_{\text{ref}}(r) = g'_{\text{ref}}(0)r + o(r) \quad (\text{A5})$$

Therefore

$$\begin{aligned} \beta V(r) g_{\text{ref}}(r) &= -L^2 \beta \epsilon a e^{-r/a} g'_{\text{ref}}(0) + o(1) = \\ &= -36 \beta \epsilon \Delta^4 R_g^4 \frac{e^{-r/a}}{a^3} g'_{\text{ref}}(0) + o(1) \quad (\text{A6}) \end{aligned}$$

where  $R_g^2 = L\sigma^2/6$  has been used. Now, taking the limit  $a \rightarrow 0$ , we find

$$\lim_{a \rightarrow 0} \beta V(r) g_{\text{ref}}(r) = -288 \pi \beta \epsilon \Delta^4 R_g^4 g'_{\text{ref}}(0) \delta(\mathbf{r}) \quad (\text{A7})$$

since the contribution of the  $o(1)$  in (A6) goes to zero. The RMPY/HTA closure relation hence reduces to

$$C_{\text{mm}}(r) = \tilde{c}_0 \left(1 - \frac{\Theta}{T}\right) R_g^3 \delta(\mathbf{r}) \quad (\text{A8})$$

with the temperature  $\Theta$  given by

$$\Theta = -288 \pi \Delta^4 \frac{g'_{\text{ref}}(0) R_g}{\tilde{c}_0} \frac{\epsilon}{k_B} \quad (\text{A9})$$

(remember that  $\tilde{c}_0 < 0$ , as seen in eq A2). The latter expression can be greatly simplified; using the fact that, for large  $q$ ,  $\hat{h}_{\text{ref}}(q)$  decays like  $4\tilde{c}_0/(q^4 R_g)$ , this allows us to show that

$$g'_{\text{ref}}(0) = -\frac{\tilde{c}_0}{2\pi R_g} \quad (\text{A10})$$

which yields

$$\Theta = 144 \Delta^4 \frac{\epsilon}{k_B} \quad (\text{A11})$$

Thus, we find that  $\Theta$  is the same for both choices of the polymer form factors, eqs 4 or 5, and is independent of the polymer density. Fourier transforming  $C_{\text{mm}}(r)$ , defining  $\tilde{c}$  as in eq 7, and injecting the result in eq 3, one obtains eq 6.

As anticipated by its notation,  $\Theta$  is in fact the  $\theta$  temperature of the present polymer model. This can be first seen from eq A8, since one finds that  $C_{\text{mm}}(r)$ , often interpreted as a renormalized two-body monomer–monomer interaction, vanishes for  $T = \Theta$ . More evidently, this can be shown by considering the pressure of the polymer fluid. Following the “compressibility route”,<sup>25</sup> the pressure is indeed easily calculated to be

$$\begin{aligned} \beta P &= \int_0^\rho (1 - \rho' \hat{C}_{\text{mm}}(q=0, \rho')) d\rho' = \\ &= \rho - \left(1 - \frac{\Theta}{T}\right) R_g^3 \int_0^\rho \rho' \tilde{c}_0(\rho') d\rho' \quad (\text{A12}) \end{aligned}$$

and one sees that, for  $T = \Theta$ , the pressure is that of a perfect gas, meaning in particular that its second virial coefficient vanishes, which is the usual definition of the  $\theta$  temperature.

Here again, a fully analytic expression for  $h_{\text{mm}}(r)$  can be obtained if the Padé approximant of the chain form factor is used. It retains the form of A3, with  $\xi_c$  unchanged and  $\xi_\rho = R_g/(2(1 - \rho \tilde{c} R_g^3))^{1/2}$ .

### 3. Relation to the Theory of Chatterjee and Schweizer.

We show here that the present calculation is related to an asymptotic regime of the theory developed in refs 15 and 16 in which the range of the attractive tail was kept finite. To this purpose, the calculation of the pressure is considered.

In refs 15 and 16 where the approximate chain-form factor (5) was used, the pressure was found to be given by (see eq 30 of ref 15)

$$\begin{aligned} \beta P &= \rho + \pi(2)^{1/2} R_g^3 \rho^2 + \frac{2}{3} \pi^2 R_g^6 \rho^3 - \\ &= \beta \epsilon \left( 12 \pi (6)^{1/2} \Delta^3 R_g^3 (L)^{1/2} \rho^2 - \frac{12 \Delta^2 L \rho}{1 + (a(2)^{1/2}/R_g)} + \right. \\ &\quad \left. \frac{(6)^{1/2} \Delta L (L)^{1/2}}{\pi R_g^3} \ln \left( 1 + \frac{2 \pi (6)^{1/2} \Delta R_g^3 \rho}{(L)^{1/2} (1 + (a(2)^{1/2}/R_g))} \right) \right) \quad (\text{A13}) \end{aligned}$$

where the notations of the present paper are used and  $\sigma$  and  $\rho_m$  have been re-expressed as functions of  $L$ ,  $R_g$ , and  $\rho$ , using the relations  $R_g^2 = L\sigma^2/6$  and  $\rho_m = \rho L$ .  $a$  can be handled in a similar way, using the fact that  $R_g^2 = La^2/(6\Delta^2)$  and all the variables which vanish in the thread limit as defined in section II are then eliminated. The only remaining singular quantity is  $L$ , which should go to infinity. Taking this limit in eq A13, after a large  $L$  expansion of the logarithm and denominators is performed, leads to

$$\beta P = \rho + \pi(2)^{1/2} R_g^3 \left(1 - \frac{\Theta}{T}\right) \rho^2 + \frac{2}{3} \pi^2 R_g^6 \left(1 - \frac{\Theta}{T}\right) \rho^3 \quad (\text{A14})$$

which is precisely the result obtained by combining eqs A12 and A2. This indicates that the present theory corresponds to an  $a \rightarrow 0$  limit of the theory of Chatterjee and Schweizer.

**4. Limitations of the Model.** The present polymer theory shows some limitations which are reviewed here.

First, in the presence of attractive interactions, the hard-core condition  $h_{\text{mm}}(r=0) = -1$  is no longer enforced.<sup>15</sup> For instance, one finds for the analytic solution

$$h_{\text{mm}}(r=0) = \frac{1 - (1 - \rho \tilde{c} R_g^3)^{1/2}}{\pi(2)^{1/2} \rho R_g^3} \quad (\text{A15})$$

which is strictly larger than  $-1$  for all densities and finite temperatures. Such a feature is very common in this kind of thermodynamic perturbation-type approximations, where the direct correlation function is completely specified for all values of  $r$ . We expect its impact to be modest on the outcome of the proposed coarse-graining procedure since we will be interested in a description on a mesoscopic level, while this inaccuracy manifests itself on the microscopic, monomer level.

Second, below the  $\theta$  temperature, there is a domain where the integral equations exhibit a singularity, corresponding to the vanishing of the denominator of eq 6. This is in fact the remnant, when  $L$  goes to infinity while taking the thread limit used in this work, of the finite  $L$  spinodal instability found by Chatterjee and Schweizer,<sup>15</sup> with a critical temperature equal to  $\Theta$  and an infinite critical value of  $\rho R_g^3$ . The boundary of this low-temperature, high-density domain can be explicitly computed when the approximate expression of the form factor is used, leading to

$$\rho R_g^3 = \frac{1}{\pi(2)^{1/2}} \left( \left( \frac{\Theta}{\Theta - T} \right)^{1/2} - 1 \right) \quad T < \Theta \quad (\text{A16})$$

This means that, below the  $\theta$  temperature, where polymer solutions are known to phase separate between polymer-rich and solvent-rich fluids, the proposed theory will only allow to investigate the latter phase.

## Appendix B: Analytic Effective Pair Potential between Average Monomers

A fully analytic expression for  $\beta v_{aa}(r)$  can be obtained if the approximate expression (5) for the chain form factor is used. Indeed, the expression for  $h_{aa}(r) \equiv h_{mm}(r)$  is known; solving eq 8 for  $h_{aa}(q)$  and identifying the result with eq 6, one finds

$$\hat{c}_{aa}(q) = \frac{\tilde{c} R_g^3 \hat{\Omega}_{mm}(q)^2}{1 - \rho \tilde{c} R_g^3 \hat{\Omega}_{mm}(q) + \rho \tilde{c} R_g^3 \hat{\Omega}_{mm}(q)^2} \quad (\text{B1})$$

Replacing  $\hat{\Omega}_{mm}(q)$  by its expression (eq 5),  $\hat{c}_{aa}(q)$  and, subsequently,  $c_{aa}(r)$  are easily obtained. Two regimes are found, depending on the sign of  $\tilde{c}$ .

If  $\tilde{c} < 0$ , i.e.,  $T > \Theta$ , one finds that  $c_{aa}(r)$  is the difference between two Yukawa terms

$$c_{aa}(r) = \frac{\tilde{c}}{2\pi(\rho \tilde{c} R_g^3 (\rho \tilde{c} R_g^3 - 4))^{1/2}} \frac{e^{-r/\xi_+} - e^{-r/\xi_-}}{r/R_g} \quad (\text{B2})$$

where

$$\xi_{\pm} = \frac{R_g}{(2 - \rho \tilde{c} R_g^3 \mp (\rho \tilde{c} R_g^3 (\rho \tilde{c} R_g^3 - 4))^{1/2})^{1/2}} \quad (\text{B3})$$

If  $\tilde{c} > 0$ , i.e.,  $T < \Theta$ ,  $c_{aa}(r)$  shows damped oscillations

$$c_{aa}(r) = -\frac{\tilde{c}}{\pi(\rho \tilde{c} R_g^3 (4 - \rho \tilde{c} R_g^3))^{1/2}} \frac{e^{-r/\xi_e}}{r/R_g} \sin(r/\xi_s) \quad (\text{B4})$$

where

$$\xi_e = R_g \left( \frac{2}{4 - \rho \tilde{c} R_g^3} \right)^{1/2} \quad \xi_s = R_g \left( \frac{2}{\rho \tilde{c} R_g^3} \right)^{1/2} \quad (\text{B5})$$

Combining these results with eqs A3 and 9 provides the desired analytic expression for  $\beta v_{aa}(r)$ .

**Acknowledgment.** The authors thank A.A. Louis for useful discussions, and B.R. acknowledges financial support from the École Normale Supérieure (Paris) and Schlumberger Cambridge Research.

## References and Notes

- (1) Flory, P. J.; Krigbaum, W. R. *J. Chem. Phys.* **1950**, *18*, 1086.
- (2) Grosberg, A. Y.; Khalatur, P. G.; Kholkhov, A. R. *Makromol. Chem. Rapid Commun.* **1982**, *3*, 709.
- (3) Olaj, O. F.; Lantschbauer, W.; Pelinka, K. H. *Macromolecules* **1980**, *13*, 299.
- (4) Dautenhahn J.; Hall, C. K. *Macromolecules* **1994**, *27*, 5399.
- (5) Louis, A. A.; Bolhuis, P. G.; Hansen, J.-P.; Meijer, E. J. *Phys. Rev. Lett.* **2000**, *85*, 2522.
- (6) Bolhuis, P. G.; Louis, A. A.; Hansen, J.-P.; Meijer, E. J. *J. Chem. Phys.* **2001**, *114*, 4296.
- (7) Bolhuis, P. G.; Louis, A. A. *Macromolecules* **2002**, *35*, 1860.
- (8) Krüger, B.; Schäfer, L.; Baumgärtner, A. *J. Phys. (France)* **1989**, *50*, 319.
- (9) Krakoviack, V.; Hansen, J.-P.; Louis, A. A. *Phys. Rev. E* **2003**, *67*, 041801.
- (10) Bolhuis, P. G.; Louis, A. A.; Hansen, J.-P. *Phys. Rev. E* **2000**, *64*, 021801.
- (11) For a review, see: Schweizer, K. S.; Curro, J. G. *Adv. Chem. Phys.* **1997**, *97*, 1.
- (12) Chandler, D.; Andersen, H. C. *J. Chem. Phys.* **1972**, *57*, 1930.
- (13) Krakoviack, V.; Hansen, J.-P.; Louis, A. A. *Europhys. Lett.* **2002**, *58*, 53.
- (14) (a) Schweizer, K. S.; Curro, J. G. *Macromolecules* **1988**, *21*, 3070. (b) Schweizer, K. S.; Curro, J. G. *Macromolecules* **1988**, *31*, 3082. (c) Schweizer, K. S.; Curro, J. G. *Chem. Phys.* **1990**, *149*, 105.
- (15) Chatterjee, A. P.; Schweizer, K. S. *J. Chem. Phys.* **1998**, *108*, 3813.
- (16) Chatterjee, A. P.; Schweizer, K. S. *Macromolecules* **1998**, *31*, 2353.
- (17) Chandler, D. *Phys. Rev. E* **1993**, *48*, 2898.
- (18) Doi, M.; Edwards, S. F. *The Theory of Polymer Dynamics*; Clarendon Press: Oxford, 1986.
- (19) Fuchs, M.; Müller, M. *Phys. Rev. E* **1999**, *60*, 1921.
- (20) A very clear discussion of the thread limit can be found in: Fuchs, M.; Schweizer, K. S. *Phys. Rev. E* **2001**, *64*, 021514.
- (21) Schweizer, K. S.; Yethiraj, A. *J. Chem. Phys.* **1993**, *98*, 9053.
- (22) Jusufi, A.; Dzubiella, J.; Likos, C. N.; von Ferber C.; Löwen H. *J. Phys.: Condens. Matter* **2001**, *13*, 6177.
- (23) See: Likos, C. N. *Phys. Rep.* **2001**, *348*, 267 and references therein.
- (24) For a related idea, see: Schmidt, M. *Phys. Rev. E* **2002**, *65*, 022801.
- (25) For example, see: Hansen, J.-P.; McDonald, I. R. *Theory of Simple Liquids*; Academic Press: London, 1986.
- (26) In this practical calculation, the order of the operations of monomer averaging and effective potential calculation has been inverted, compared to the description of the process given before. In the limit of very long chains where end effects are negligible, this should be harmless. However, there is no reason to think that in general these two operations commute and this could lead to subtle effects, for short chains for instance.
- (27) (a) Lang, A.; Likos, C. N.; Watzlawek, W.; Löwen, H. *J. Phys.: Condens. Matter* **2000**, *12*, 5087. (b) Louis, A. A.; Bolhuis, P. G.; Hansen, J.-P. *Phys. Rev. E* **2000**, *62*, 7961. (c) Louis, A. A. *Philos. Trans. R. Soc. London A* **2001**, *359*, 939. (d) Likos, C. N.; Hoffmann, N.; Löwen, H.; Louis, A. A. *J. Phys.: Condens. Matter* **2002**, *14*, 7681.
- (28) Müller, M.; Binder, K.; Schäfer, L. *Macromolecules* **2000**, *33*, 4568.
- (29) For  $\rho \equiv 0$ ,  $\beta v_{aa}(r) = -\ln(1 - e^{-r/\xi_e})$  and thus decays only exponentially for large  $r$ . However, for all cases of interest, the polymer density is finite and this marginal behavior is of little relevance.
- (30) The impossibility to properly identify the domain of existence of the low-density phase below  $\Theta$  is a consequence of the version of the thread PRISM theory considered in this work, which implements the limits  $L \rightarrow \infty$ ,  $d, \sigma$ , and  $a \rightarrow 0$  in a strict sense. As can be seen in Appendix A in the case of the spinodal line, this rejects the liquid branch to infinite polymer density and thus prevents a meaningful investigation of liquid–gas coexistence. This was not the case in ref 15, where complete phase diagrams, including both spinodals and binodals, could be obtained.
- (31) (a) Koyama, R. *Makromol. Chem.* **1980**, *181*, 1987. (b) Koyama, R. *Macromolecules* **1981**, *14*, 1299.
- (32) (a) Guenza, M. *Phys. Rev. Lett.* **2002**, *88*, 025901. (b) Guenza, M. *Macromolecules* **2002**, *35*, 2714.
- (33) Tanaka, F. *J. Chem. Phys.* **1985**, *82*, 4707.
- (34) Czech, R.; Hall, C. K. *Macromolecules* **1991**, *24*, 1535.
- (35) Grosberg, A. Y.; Kuznetsov, D. V. *Macromolecules* **1992**, *25*, 1991.
- (36) Raos, G.; Allegra, G. *Macromolecules* **1996**, *29*, 6663.
- (37) Upon inversion of the low-density simulation data of Figure 5 for chains of length  $L = 500$ , the resulting effective c.m.–c.m. pair potential does not show a repulsive short-range component. This tends to support the possibility that this repulsion is a short-chain artifact, but a more systematic study in temperature and density would be necessary to reach a final conclusion.